

White Paper  
**Miniature Atomic Clock (MAC) Pre-Production Results**



## Abstract

---

The authors have developed a miniature atomic clock (MAC) for applications requiring atomic timing accuracy in portable battery-powered applications. Recently, we have completed a pre-production build of 10 devices in order to evaluate unit-to-unit performance variations and to gain statistical confidence in the performance specifications, environmental sensitivity, and manufacturability.

## The Miniature Atomic Clock (MAC)

Atomic clocks play an essential role in the precise timing and synchronization of modern communications and navigation systems. To date, the relatively large size and power consumption of existing technologies have prevented the deployment of atomic clocks in portable, battery-powered applications. However, the demand for high-precision timing in portable devices is steadily increasing for applications in broadband and secure communications and precise location and navigation systems.

Since 2002, the authors have been developing a Chip Scale Atomic Clock (CSAC), with an emphasis on small size, low power, and batch fabrication techniques for lower cost. At the 2005 Frequency Control Symposium, we reported on the demonstration of a prototype MAC, with an overall size of 10 cm<sup>3</sup>, power consumption <200 mW and short-term stability,  $\sigma_y(\tau) < 1 \times 10^{-9}\tau^{-1/2}$  <sup>1</sup>. The reader is referred to that paper for additional references, which describe in detail the fundamental research and design tradeoffs that underlie the evolution of the current design.

Since our previous report, we have continued the development of the prototype MAC to improve performance, usability, and manufacturability. In particular, the short-term stability has been improved by a factor of two, the power consumption has been reduced to 125 mW, and the microwave synthesizer has been redesigned to allow for a precise calibrated output at 10.0 MHz. The firmware has evolved to provide for autonomous acquisition and operation, internal state-of-health determination, and remote calibration and status monitoring.

In this paper, we review the MAC architecture, with particular attention to those aspects which have changed since our previous report, as well as the results of testing of 10 prototype MACs, including short-term stability, frequency drift, temperature coefficient, and power-on retrace.

### Architecture

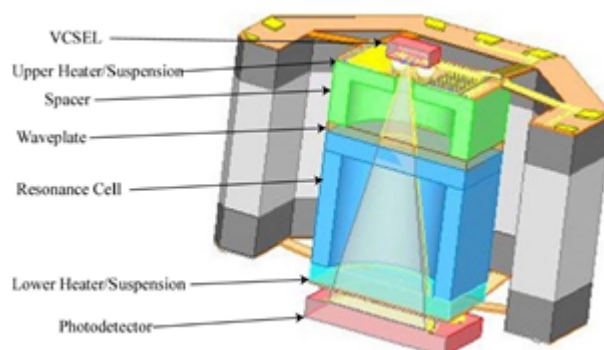
In order to achieve compact size and low-power operation, the MAC physics package interrogates the cesium hyperfine resonance with the technique of coherent population trapping (CPT) rather than the microwave double-resonance scheme employed in conventional vaporcell atomic clocks<sup>2,3,4</sup>. Interrogation of the CPT resonance is accomplished by the application of a coherently bichromatic optical field, near to the cesium “D1” transition at 894 nm, which is produced by modulating the bias current of a high-bandwidth vertical-cavity surface-emitting laser (VCSEL) at one-half of the ground state hyperfine frequency,  $\nu_0/2 \approx 4.6$  GHz. The advantages of this interrogation scheme include the elimination of the high power RF discharge lamp and tuned microwave cavity of the conventional design.

The choice of cesium over rubidium is dictated by the higher vapor density of cesium, which leads to lower operating power, and by the superior reliability of VCSELs at cesium wavelengths.

### Physics Package

The following illustration shows the MAC physics package.

**Figure 1 • Second-Generation Physics Package**



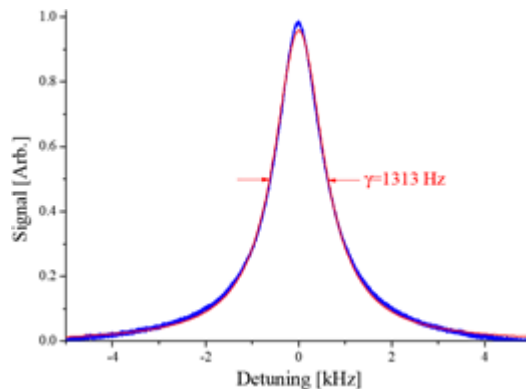
The second-generation physics package includes the major elements of the successful prototype design described previously with several improvements that enhance its performance and manufacturability<sup>5, 6</sup>.

The essential elements of the physics package are the resonance cell, shown in blue, and the VCSEL and photodetector, located above and below the resonance cell respectively. The resonance cell is comprised of a silicon body (2 mm square and 2 mm thick) with anodically-bonded transparent Pyrex® windows, following the technique pioneered by Liew<sup>7</sup>. The sealed cell contains a small amount of metallic cesium as well as a temperature-compensating mixture of buffer gases. The VCSEL is mounted on the upper suspension, which is spaced from the cell to allow divergence prior to the cell in order to reduce the inhomogeneous light shift and effectively illuminate the cell volume. A custom low-threshold high-bandwidth VCSEL, operating at the cesium D1 wavelength of  $\lambda = 894.3$  nm was developed specifically for this application<sup>8</sup>. The choice of the D1 wavelength rather than the more readily available D2 wavelength ( $\lambda = 852.4$  nm) is dictated by the superior CPT signal quality at the D1 wavelength<sup>9, 10</sup>. Immediately prior to entering the resonance cell, the VCSEL beam passes through a quarterwave retarder, oriented with its principal axis at 45° to the laser polarization in order to generate a circularly-polarized field in the interaction volume.

The physics assembly is temperature stabilized at  $\approx 85$  °C to generate sufficient cesium vapor pressure and to stabilize the wavelength of the VCSEL. The power constraints of the MAC thus demand a high degree of thermal isolation between the physics package and the ambient thermal environment. Vacuum-sealing the entire physics assembly eliminates the predominant mode of thermal loss, which is conduction and convection through the gaseous ambient. The cell is suspended, above and below, by a pair of strained polyimide suspensions, which provide both thermal isolation and mechanical support. Resistive platinum heaters, as well as the electrical connections to the optoelectronic components, are patterned onto the polyimide, which permits their mechanical dimensions, and thus their thermal conductivity to be determined by electrical rather than mechanical requirements. The dominant heat loss mechanism from the physics assembly is thus thermal radiation from the heated area to the surrounding package.

In normal operation, the physics package is heated to  $\approx 85$  °C in a 25 °C ambient, requiring approximately 10 mW of heater power. The temperature, VCSEL bias current, and microwave power are then adjusted to optimize the CPT resonance signal, as shown in the following illustration.

**Figure 2 • CPT Resonance**

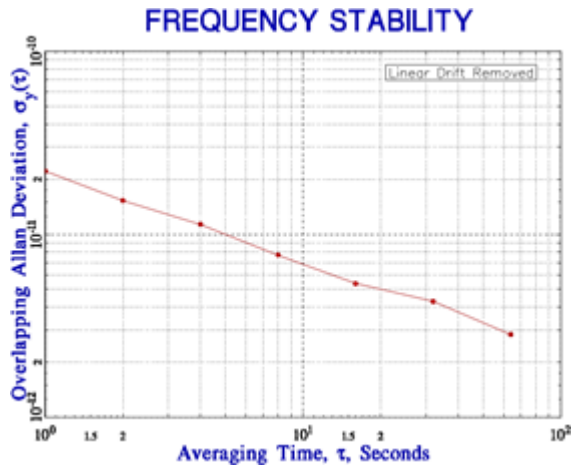


**Note:** Red—data, Blue—Lorentzian fit

The line width of the CPT resonance is  $\gamma \approx 1300$  Hz and the contrast (measured as CPT amplitude divided by the DC light level) is typically  $\approx 1\%$ .

The following illustration shows typical short-term frequency stability of a MAC physics package, measured with optimal laboratory scale electronics.

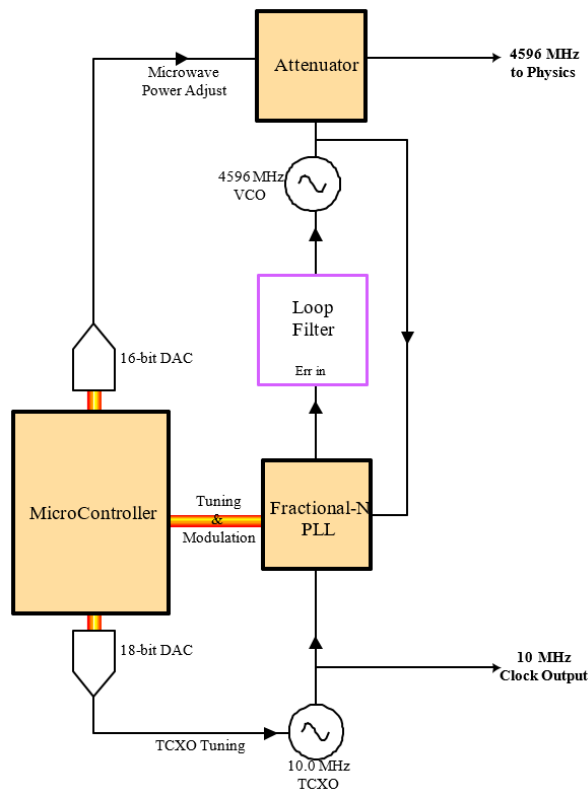
Figure 3 • MAC Physics Package Frequency Stability



All 10 of the physics packages built for the MAC prototypes have demonstrated short-term stability, measured in this optimal fashion, of  $\sigma_y(\tau) < 1 \times 10^{-10} \tau^{-1/2}$ , with most falling into the range of  $\sigma_y(\tau) = 2-4 \times 10^{-11} \tau^{-1/2}$ .

### Microwave Synthesis

The functional purpose of the MAC microwave synthesizer is to simultaneously provide a spectrally pure clock output at 10.0 MHz along with a coherently synthesized tunable source at 4.596 GHz for the atomic interrogation. The following illustration shows a block diagram for the MAC microwave synthesizer.

**Figure 4 • Microwave Synthesizer**

The microwave synthesizer consists of a 4596 MHz voltage-controlled oscillator (VCO), which is phase-locked to a 10 MHz temperature-compensated crystal oscillator (TCXO) through a low-power fractional-N phase-locked loop (PLL) integrated circuit. The frequency multiplication factor, between the TCXO and VCO, can be varied, under microprocessor control, with a resolution of 2 parts in  $10^{12}$ . A voltage-controlled attenuator at the 4.6 GHz output of the synthesizer allows for precise microprocessor control of the microwave amplitude applied to the physics package.

## Control Electronics

The MAC control electronics are relatively simple, compared to conventional atomic clocks. In order to minimize component count, and thereby size and power consumption, many of the analog functions of traditional atomic clock architecture are implemented algorithmically in the MAC firmware. In addition to the physics package, the system consists principally of a microprocessor, multiple channels of analog input (ADC) and output (DAC), and the microwave synthesizer. The MAC operates from a single external 3.3 V supply, with internal regulators providing secondary regulation to 3.0 V and 2.8 V for the analog signal chain and the microwave synthesizer, respectively.

The following illustration shows the complete MAC electronics. The physics package, with the vacuum lid removed, is on the right.

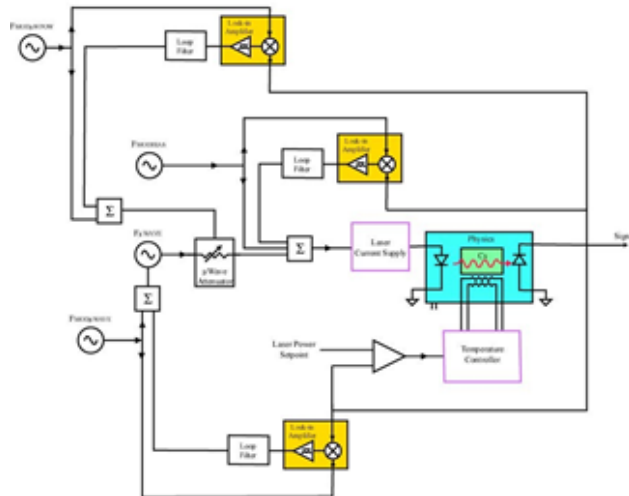
**Figure 5 • MAC Electronics**



## Firmware

Much of the complexity of the MAC control systems are implemented in firmware. The following illustration shows a block diagram of the servo systems.

**Figure 6 • Block Diagram of the MAC Servos**



Multiple servos are implemented in the firmware in order to simultaneously stabilize the temperature of the physics package, the laser bias current, the microwave power, and the clock frequency. Insofar as possible, these controls are servoed to measurements of atomic properties within the physics package. This approach stabilizes the characteristics of the CPT resonance and thus the clock frequency against long-term drift and environmental perturbations. Because there is only a single signal emerging from the physics package the multiple servos are operated at different frequencies (frequency-division multiplexing) and/or at different times (time-division multiplexing). The multiple phase-synchronous detectors (in yellow in the previous illustration) are implemented entirely in firmware.

Upon initial start-up, the firmware is responsible for initial optimization of the physics package temperature and microwave power and acquisition of the optical and microwave resonances. The firmware also provides internal parameter monitoring and an RS232 telemetry interface which allows for external monitoring of internal MAC operating parameters and alarm status and for providing input of precise frequency adjustment (calibration).

## Power Budget

The following table lists the MAC power budget.

**Table 1 • MAC Power Budget**

System	Component	Power
Signal processing	MicroController	20 mW
	16-bit DACs	13 mW
	Analog	8 mW
Physics	Heater power	7 mW
	VCSEL power	3 mW
	C-Field	1 mW
Microwave/RF	4.6 GHz VCO	32 mW
	PLL	20 mW
	10 MHz TCXO	7 mW
	Output buffer	1 mW
Power regulation and passive losses		13 mW
Total		125 mW



## MAC Performance

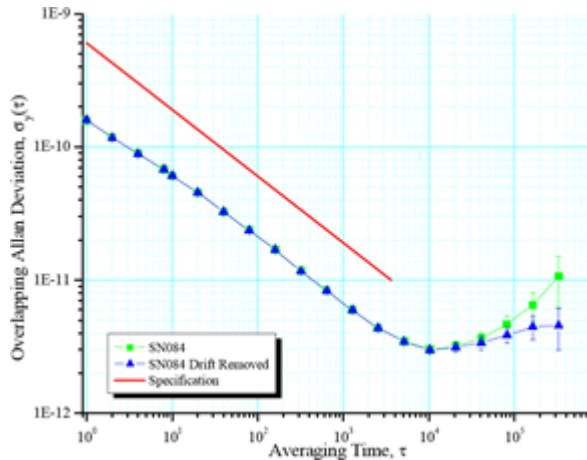
In total, 15 MACs have been built and tested, including two engineering units and 13 pre-production units. The first engineering unit, SN084, has been extensively characterized while the second, SN087, was used as a testbed for hardware and firmware development. The subsequent 13 units, with serial numbers of the form SN3xx, were subjected to standard acceptance tests prior to delivery to proof-of-concept applications. Of these, three consecutive units (SN320–322) failed prematurely due to VCSEL failure. These three VCSELs were part of the same lot of four and thus we believe that these may have suffered latent damage due to electrostatic discharge (ESD) in process or handling.

### Short-Term Stability

Compared to the optimal laboratory-scale electronics used to independently measure the physics package performance, as shown in [MAC Physics Package Frequency Stability \(see page 5\)](#), some compromise in performance is expected with the low-power MAC electronics. In particular, the short-term stability of the MAC is degraded by noise on the VCSEL bias current and by phase noise on the microwave synthesizer.

The following illustration shows the Allan deviation of MAC SN084 for a 3-week data period.

**Figure 7 • MAC SN084 Stability**

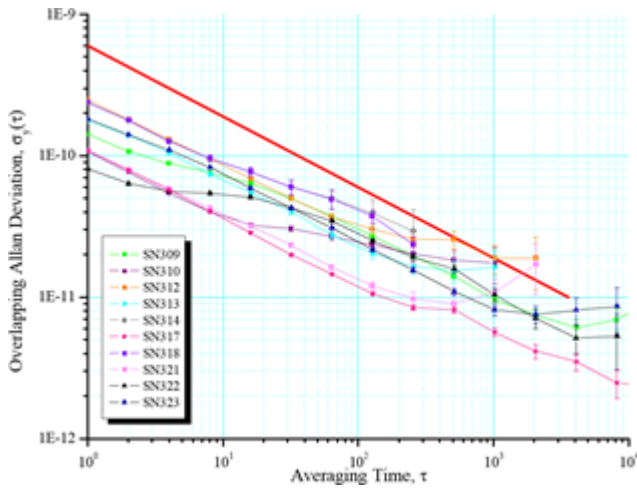


SN084 is unique among the prototypes in that it has been operated for nearly 200 days and, as such, the frequency drift rate is relatively low ( $<1 \times 10^{-11}$ /day). The plot shows the specification (in red) along with the measured instability with and without the linear drift removed (in blue and green, respectively).

The short-term stability performance of SN084 is  $\sigma_y(\tau) \approx 1.5 \times 10^{-10}\tau^{-1/2}$ , which is typical for all of the units built and tested to date.

The following illustration shows the stability data for 10 pre-production prototype MACs.

**Figure 8 • Collected STS Data for 10 MACs**

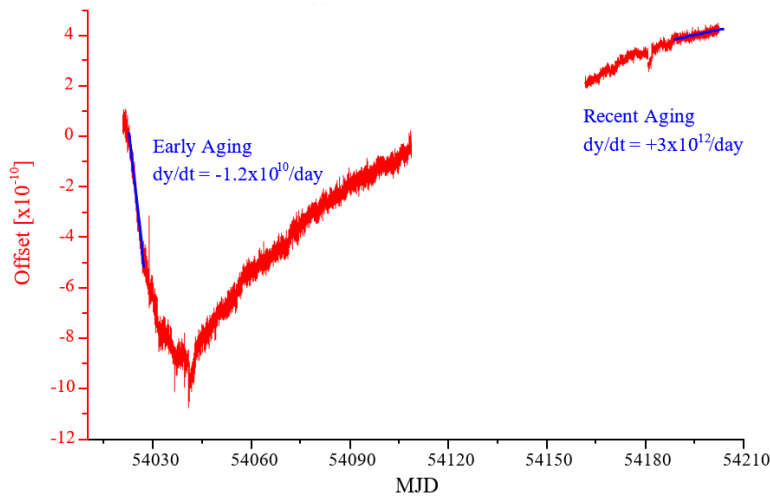


All units exhibit  $\sigma_y(\tau) < 3 \times 10^{-10}\tau^{-1/2}$  out to averaging intervals of  $\tau > 100$  seconds. Because the phase data was collected shortly after assembly, linear drift was removed from the frequency data prior to the calculation of Allan deviation. Nonetheless, the long-term stability of the deliverable units diverges from ideal behavior at longer averaging times, principally due to early non-linear aging effects.

### Long-Term Drift

The long-term frequency behavior of the engineering unit, SN084, has been monitored for  $\approx 200$  days. The measured frequency is shown in the following illustration.

**Figure 9 • Long-Term Aging of SN084**



The data in the previous illustration is pieced together from several data sets, including several unintentional power outages and a 45-day interruption during which the unit was removed from aging in order to update the electronics and firmware to the latest revision. Arbitrary frequency offsets were applied at Modified Julian Date (MJD) 54161 and MJD 54180 in order to realign the aging data.

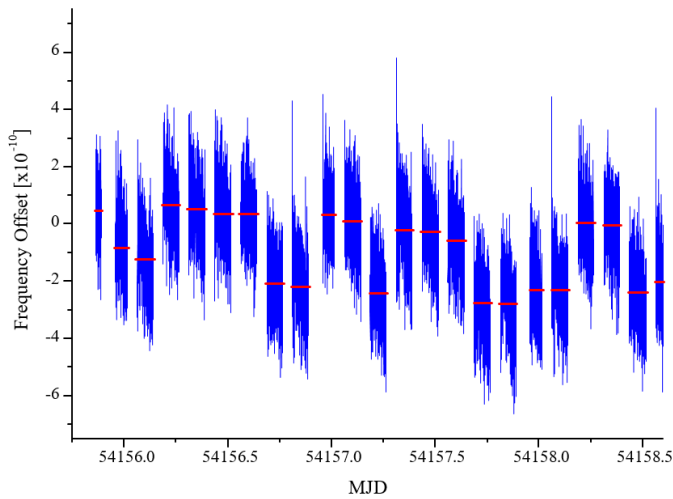
The shape of the aging curve for SN084 appears to be typical for most of the evaluated MACs but we do not have a long data record for any other unit than SN084. Initially, the aging is fairly large ( $\approx 1.2 \times 10^{-10}/\text{day}$ ) and negative. Following approximately two weeks of negative aging, the aging changes sign and begins a cycle of exponentially-decaying positive aging. Towards the end of the data record, following 200 days of operation, the aging rate has reduced to  $\approx +3 \times 10^{-12}/\text{day}$  ( $\approx 1 \times 10^{-10}/\text{month}$ ).

### Retrace

Retrace is defined to be the frequency error due to power-cycling the unit. In our laboratory, retrace is measured by periodically powering the unit from a household security timer while monitoring the frequency output.

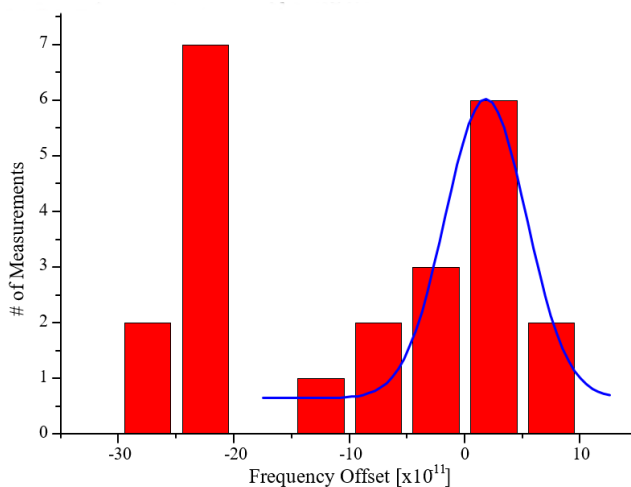
The following illustration shows a typical retrace measurement, during which MAC SN312 was cycled with a 2-hour on/1-hour off duty cycle. The blue trace is measured data and the red lines indicate the mean value of the frequency offset in each measurement interval.

Figure 10 • MJD



The following illustration shows the frequency measurements.

Figure 11 • Histogram of Retrace Values from MJD



It is clear from the data in the previous two illustrations that the retrace behavior is bimodal. This reflects a shortcoming of the current MAC implementation. Including both retrace modes, the retrace (FWHM) is about  $\Delta y = 2\text{--}3 \times 10^{-10}$ , whereas the retrace within a single mode (shown in blue) is only  $\Delta y = 7 \times 10^{-11}$ . To varying extents, this behavior is typical of all 10 of the prototype MACs. In each case, the retrace of either mode is  $\Delta y < 1 \times 10^{-10}$ , while the splitting between the modes is typically  $\Delta y \approx 1 \times 10^{-10}$  (as in SN312, shown previously). In the worst case the modes are separated by  $\Delta y \approx 1 \times 10^{-9}$ .

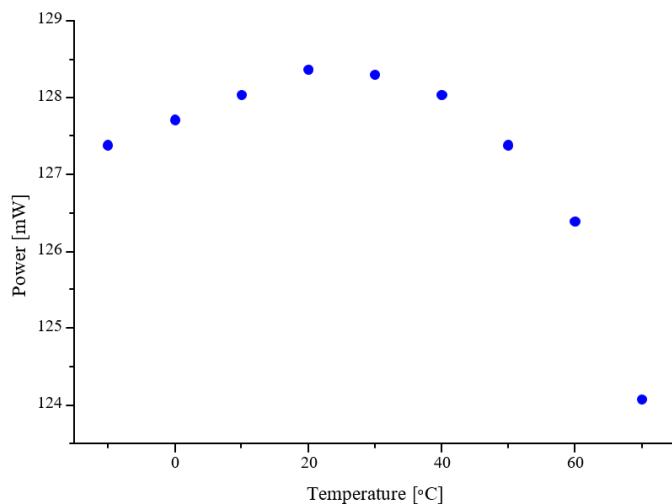
We suspect that the bimodal retrace behavior is the result of the VCSEL starting up randomly in either the x or y linear polarization state. In typical VCSELs (including Microsemi), there is no strong anisotropy to select one linear polarization state over the orthogonal state. We have historically relied on a small amount of crystal strain, due to the fabrication or packaging processes, to break the symmetry and preferentially select a single operating polarization<sup>11</sup>. Modifications in our fabrication and/or packaging procedures have possibly reduced the amount of strain experienced by our VCSELs, causing less polarization discrimination. One potential long-term solution would be to fabricate VCSELs using shallow surface gratings to provide stronger polarization discrimination<sup>12</sup>. In the meantime, the cause and potential cures for the bimodal retrace remain under investigation.

## Performance over Temperature

In real world applications, the MACs may be subjected to temperature variations of  $\pm 10^\circ\text{C}$  and most require qualification over a range of  $\Delta T = 0^\circ\text{C}\text{--}50^\circ\text{C}$ , or wider. In extreme temperature applications, the key parameters are power consumption and frequency change with temperature.

Because of the extraordinary thermal isolation of the physics package, the power consumption of the MAC is relatively insensitive to ambient temperature, compared to conventional atomic clocks. At lower operating temperatures, the physics package requires slightly more heater power (roughly  $1\text{ mW}/7^\circ\text{C}$ ) but other components, such as the microprocessor, run more efficiently. The upper temperature limit is determined by the requirement to temperature-stabilize the physics package at  $\approx 85^\circ\text{C}$ . Even with the heaters turned off, the VCSEL dissipates  $\approx 2\text{ mW}$ , which limits the upper operating ambient to  $T \approx 70^\circ\text{C}$ .

**Figure 12 • MAC Power Consumption vs. Ambient Temperature**

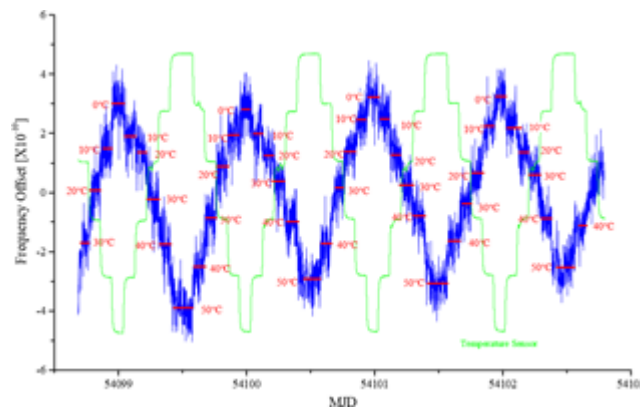


The following illustration shows the MAC power consumption as a function of ambient temperature. It is not surprising that the power consumption decreases by several milliWatts at elevated ambient (roughly  $1\text{ mW}/7^\circ\text{C}$ ) from  $40^\circ\text{C}\text{--}70^\circ\text{C}$ . It is surprising, though, that the power continues to drop at lower temperatures, indicating that the power savings of cooling the other electronic components offsets the increased heater power required by the physics package. In general, the power consumption changes by only 1%–2%, from the nominal 125 mW, over the nominal operating range of  $0^\circ\text{C}\text{--}50^\circ\text{C}$ .

The frequency change of the MAC over temperature is caused by several different and interacting sources that affect the frequency of the cesium CPT resonance. The principal sources of CPT temperature coefficient are changes in the buffer gas and the laser spectrum, which impact the collisional shift and AC Stark shift, respectively. In order to reduce the effects of the buffer gas collisions, the resonance cell is filled with a mixture of two buffer gases, argon and nitrogen, which produce oppositely signed shifts of the resonance line ( $-191$  Hz/Torr and  $+924$  Hz/Torr, respectively)<sup>13</sup>. Spectral variations are minimized, insofar as possible, by the servos, which stabilize the DC power of the VCSEL and optimize the microwave modulation amplitude. Nonetheless, there remains some temperature coefficient in the MAC, due to second-order buffer gas effects, spectral changes due to thermal gradients in the physics package, which change the DC bias point of the VCSEL, and other electronic effects, such as variation of the magnetic bias field circuit.

The following illustration shows the frequency offset of MAC SN310 (in blue) as the temperature is cycled from  $0\text{ }^{\circ}\text{C}$ – $50\text{ }^{\circ}\text{C}$ – $0\text{ }^{\circ}\text{C}$ , in  $10$ -degree steps, with a two-hour dwell at each temperature. The temperature measured by the MAC internal temperature sensor (in green) and the average frequency offset in each measurement (in red).

**Figure 13 • Uncompensated MAC Temperature Performance**

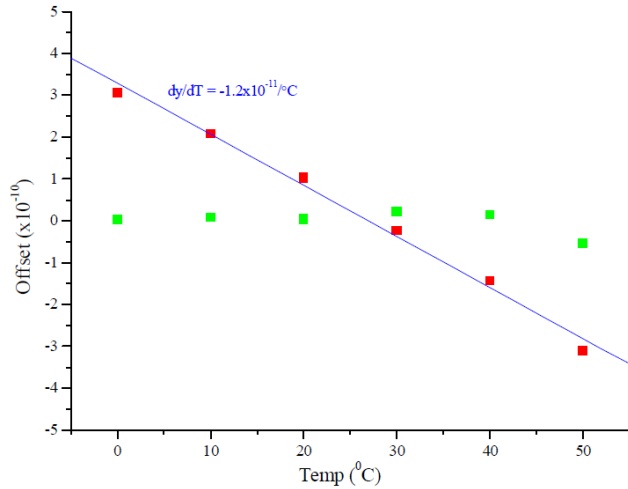


Over the measurement range of  $0\text{ }^{\circ}\text{C}$ – $50\text{ }^{\circ}\text{C}$ , the MAC exhibits an approximately linear variation of  $\Delta y/\Delta T \approx 8 \times 10^{-10}/50\text{ }^{\circ}\text{C}$ .

The reproducible and nearly linear temperature response, shown in the previous illustration, along with the high correlation to the internal temperature sensor reading provides a mechanism for digital temperature compensation. The temperature coefficient of each unit is individually calibrated over temperature with respect to the internal temperature sensor measurement. In normal operation, the temperature sensor is continuously monitored and a small correction is applied to the microwave synthesizer.

The following illustration shows the improvement in temperature performance resulting from digital compensation.

**Figure 14 • MAC Frequency Offset vs. Temperature with (green) and Without (red) Active Compensation**

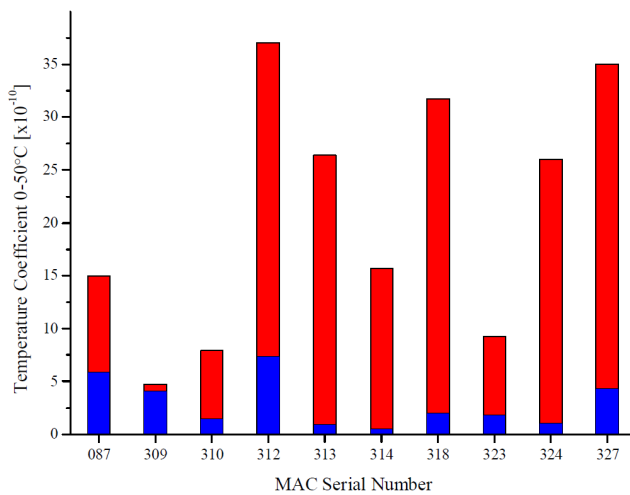


The red points are the average values extracted from the measurement of [Collected STS Data for 10 MACs \(see page 10\)](#), along with a (blue) linear fit. The green points are extracted from a similar measurement on the same unit with the active compensation enabled. With compensation enabled, the temperature coefficient is no longer linear and has been reduced by approximately one order of magnitude to  $\Delta y/\Delta T \approx 4 \times 10^{-11}/50 \text{ }^\circ\text{C}$ .

In order for the compensation to be effective, not only must the measured (uncompensated) frequency be highly correlated with the reading from the onboard temperature sensor but, in addition, the correlation must be reproducible over many cycles, power-on retrace, and independent of whether the temperature is ramping up or down.

The following illustration shows the collected 0 °C–50 °C temperature coefficient for 10 of the MACs, without compensation (red) and with compensation enabled (blue).

**Figure 15 • 0 °C–50 °C Temperature Coefficient of 10 MACs with Compensation Enabled and Disabled**



Uncompensated, most behave similarly to [Uncompensated MAC Temperature Performance \(see page 13\)](#), with temperature-driven frequency errors in the range of  $\Delta y/\Delta T \approx 1-4 \times 10^{-9}/50 \text{ }^\circ\text{C}$ . As the previous illustration shows, the compensation works fairly well for most units, reducing the temperature coefficient to  $\Delta y/\Delta T < 5 \times 10^{-10}/50 \text{ }^\circ\text{C}$ . For several units, the correlation between the uncompensated frequency change and the onboard temperature sensor is relatively poor, so that the compensation provides little, if any improvement. One unit in particular, SN309, exhibits poor symmetry between upgoing temperature changes and down-going temperature changes, perhaps reflecting a thermal discontinuity within the physics package. Nonetheless, the average temperature coefficient for the 10 units shown in the previous illustration is  $\Delta y/\Delta T = 3 \times 10^{-10}/50 \text{ }^\circ\text{C}$ .

## Conclusion

---

We have built and tested 10 prototype miniature atomic clocks, with volume  $\approx 15 \text{ cm}^3$  and power consumption  $\approx 125 \text{ mW}$ . All 10 devices exhibit excellent short-term stability of  $\sigma_y(\tau) < 3 \times 10^{-10} \tau^{-1/2}$ . Over a temperature range of  $0 \text{ }^\circ\text{C}$ – $50 \text{ }^\circ\text{C}$ , the power varies by  $< 5 \text{ mW}$  and the frequency offset changes by  $\Delta y < 4 \times 10^{-10}$ . The frequency drift, based on long-term measurements of a single unit, is better than  $1 \times 10^{-10}$ /month, after 200 days of operation. Most units exhibit a bimodal retrace behavior, which is attributed to nearly degenerate polarization modes of the VCSEL.



## References

---

- [1] R. Lutwak, et. al., “The MAC - a Miniature Atomic Clock,” *Proceedings of the 2005 International Frequency Control Symposium*, August 29-31, 2005, Vancouver, BC, pp. 752–757.
- [2] R. Lutwak, D. Emmons, W. Riley, and R.M. Garvey, “The ChipScale Atomic Clock – Coherent Population Trapping vs. Conventional Interrogation”, *Proceedings of the 34th Annual Precise Time and Time Interval (PTTI) Systems and Applications Meeting*, December 3-5, 2002, Reston, VA, pp. 539-550.
- [3] J. Kitching, et. al, *IEEE Trans. Instrum. Meas.* 49, 1313 (2000).
- [4] N. Cyr, M. Têtu, and M. Breton, *IEEE Trans. Instrum. Meas.* 42, 640 (1993).
- [5] R. Lutwak, et. al., “The Chip-Scale Atomic Clock – Low-Power Physics Package”, *Proceedings of the 36th Annual Precise Time and Time Interval (PTTI) Systems and Applications Meeting*, December 79, 2004, Washington, DC, pp. 339-354.
- [6] M. Mescher, R. Lutwak, and M. Varghese, “An Ultra-Low-power Physics Package for a Chip-Scale Atomic Clock,” *Transducers '05, IEEE International Conference on Solid-State Sensors and Actuators*, June 5-9, 2005, Seoul, KoreaS.
- [7] L-A. Liew, et. al. “Microfabricated alkali atom vapor cells,” *Applied Physics Letters*, 84, p. 2694 (2004).
- [8] D.K. Serkland, et. al. “VCSELs for Atomic Sensors,” *Proceedings of the SPIE*. Vol. 6484, 2007.
- [9] R. Lutwak, D. Emmons, W. Riley, and R.M. Garvey, “The ChipScale Atomic Clock – Coherent Population Trapping vs. Conventional Interrogation”, *Proceedings of the 34th Annual Precise Time and Time Interval (PTTI) Systems and Applications Meeting*, December 3-5, 2002, Reston, VA, pp. 539-550.
- [10] S. Knappe, J. Kitching, L. Hollberg, and R. Wynands, *Appl. Phys. B* 74, 217 (2002)
- [11] T. Mukaihara, F. Koyama, K. Iga, “Engineered polarization control of GaAs/AlGaAs surface-emitting lasers by anisotropic stress from elliptical etched substrate hole,” *IEEE Photon. Technol. Lett.*, vol. 5, pp. 133-135 (1993).
- [12] P. Debernardi, J. M. Ostermann, M. Feneberg, C. Jalics, and R. Michalzik, “Reliable polarization control of VCSELs through monolithically integrated surface gratings: a comparative theoretical and experimental study,” *IEEE J. Sel. Top. Quant. Electron.*, vol. 11, pp. 107-116 (2005).
- [13] F. Strumia, N. Beverini, A. Moretti, “Optimization of the Buffer Gas Mixture for Optically Pumped Cs Frequency Standards,” *Proceedings of the 30th Annual Symposium on Frequency Control*, June 2-4, 1976

**Microsemi Corporate Headquarters**

One Enterprise, Aliso Viejo,  
CA 92656 USA  
Within the USA: +1 (800) 713-4113  
Outside the USA: +1 (949) 380-6100  
Fax: +1 (949) 215-4996  
Email: [sales.support@microsemi.com](mailto:sales.support@microsemi.com)  
[www.microsemi.com](http://www.microsemi.com)

© 2017 Microsemi Corporation. All rights reserved. Microsemi and the Microsemi logo are trademarks of Microsemi Corporation. All other trademarks and service marks are the property of their respective owners.

Microsemi makes no warranty, representation, or guarantee regarding the information contained herein or the suitability of its products and services for any particular purpose, nor does Microsemi assume any liability whatsoever arising out of the application or use of any product or circuit. The products sold hereunder and any other products sold by Microsemi have been subject to limited testing and should not be used in conjunction with mission-critical equipment or applications. Any performance specifications are believed to be reliable but are not verified, and Buyer must conduct and complete all performance and other testing of the products, alone and together with, or installed in, any end-products. Buyer shall not rely on any data and performance specifications or parameters provided by Microsemi. It is the Buyer's responsibility to independently determine suitability of any products and to test and verify the same. The information provided by Microsemi hereunder is provided "as is, where is" and with all faults, and the entire risk associated with such information is entirely with the Buyer. Microsemi does not grant, explicitly or implicitly, to any party any patent rights, licenses, or any other IP rights, whether with regard to such information itself or anything described by such information. Information provided in this document is proprietary to Microsemi, and Microsemi reserves the right to make any changes to the information in this document or to any products and services at any time without notice.

Microsemi Corporation (Nasdaq: MSCC) offers a comprehensive portfolio of semiconductor and system solutions for aerospace & defense, communications, data center and industrial markets. Products include high-performance and radiation-hardened analog mixed-signal integrated circuits, FPGAs, SoCs and ASICs; power management products; timing and synchronization devices and precise time solutions, setting the world's standard for time; voice processing devices; RF solutions; discrete components; enterprise storage and communication solutions; security technologies and scalable anti-tamper products; Ethernet solutions; Power-over-Ethernet ICs and midspans; as well as custom design capabilities and services. Microsemi is headquartered in Aliso Viejo, California, and has approximately 4,800 employees globally. Learn more at [www.microsemi.com](http://www.microsemi.com).

MSCC-0104-WP-01001-1.00-0717